Solar Energy Materials and Solar Cells 192 (2019) 36–43

Contents lists available at ScienceDirect

Solar Energy Materials and Solar Cells

journal homepage: www.elsevier.com/locate/solmat

Damage to passivation contact in silicon heterojunction solar cells by ITO sputtering under various plasma excitation modes

Anh Huy Tuan Le[a,b], Vinh Ai Dao[c], Duy Phong Pham[d], Sangho Kim[e], Subhajit Dutta[d], Cam Phu Thi Nguyen[d], Youngseok Lee[e], Youngkuk Kim[d,*], Junsin Yi[d,*]

[a] Division of Computational Physics, Institute for Computational Science, Ton Duc Thang University, Ho Chi Minh City, Vietnam
[b] Faculty of Electrical and Electronics Engineering, Ton Duc Thang University, Ho Chi Minh City, Vietnam
[c] Institute of Fundamental and Applied Sciences, Duy Tan University, Ho Chi Minh City 700000, Vietnam
[d] College of Information and Communication Engineering, Sungkyunkwan University, Suwon 440-746, Republic of Korea
[e] Department of Energy Science, Sungkyunkwan University, Suwon 440-746, Republic of Korea

ARTICLE INFO

Keywords:
Indium tin oxide
RF-superimposed DC
Surface passivation contact
Carrier lifetime
Silicon heterojunction solar cells

ABSTRACT

Analysis of damage to passivation contact in heterojunction with intrinsic thin layer (HIT) solar cells by indium tin oxide (ITO) sputtering under various plasma excitation modes such as radio frequency (RF), direct current (DC), RF-superimposed DC, pulsed DC is presented. A significant degradation of effective minority carrier lifetime of the precursor cells at both low and high-level injections after the ITO deposition by sputtering technique was observed regardless of plasma excitation modes. We found that the main reason for this degradation was mainly due to the ion flux in the sputtering plasma rather than the ion kinetic energy. On the basis of the experimental and simulated results, we attributed the degradation of surface passivation quality mainly to the damage of the amorphous-silicon/crystalline-silicon interfaces rather than that of the intrinsic hydrogenated amorphous silicon layers. This degradation could be significantly reduced by the ITO deposition at a high temperature in which a trade-off between degradation and curing step was expected to occur. The cell performance of the HIT solar cells using the ITO films deposited by various plasma excitation modes at 180 °C was subsequently discussed. The ITO films deposited by the RF-superimposed DC mode exhibited a high potential as excellent opto-electrical properties and free sputter-induced damage electrodes for HIT solar cell applications. To our best knowledge, this is the first time that the ITO films deposited by the RF-superimpose DC mode are used as electrodes in the HIT solar cells.

1. Introduction

Until now, silicon-wafer-based solar cells are dominating the solar cells market due to their high-efficiency and stability [1,2]. Many efforts to understand the fundamentals of this kind of cells and to improve the fabricating process were implemented to reach the theoretical limitation of cell efficiency. A certificated efficiency (η) of 25.6% using 143.7-cm^2-wafer was reported by Panasonic, Japan, breaking the historic 25.0% η record set by the University of New South Wales, Australia in 1999 [3,4]. Recently, this world-record η was broken by Kaneka Corporation, which reported a η of 26.6% for silicon-wafer-based solar cells using a combination of the heterojunction with intrinsic thin layer (HIT) solar cell technology and the integrated back contact design [5]. This indicates that the HIT solar cell technology has a high potential for extremely high-efficiency solar cells. Therefore, this technology is expected to have a major contribution to a further improvement of cell efficiency, and hence a remarkable reduction of cost per watt.

In comparison with conventional crystalline silicon (c-Si) solar cells, HIT solar cells offer an excellent surface passivation, a better temperature coefficient, and a lower fabrication temperature (around 200 °C) which allows for the utilization of very thin wafers without wafer warping [6,7]. One of the most differences between the HIT and conventional c-Si solar cells is the manner of charge carrier collection in which light-generated carriers pass through hydrogenated amorphous silicon (a-Si:H) based layers and transparent conductive oxide (TCO) layers before being collected by metal electrodes. Low conductivity of these a-Si:H layers is the main reason for an insufficiency of charge carrier collection with only metal electrodes. Therefore, the contacting scheme in which TCO films play a critical role in charge carrier

* Corresponding authors.
E-mail addresses: lehuytuananh@tdtu.edu.vn (A.H.T. Le), daovinhai@dtu.edu.vn (V.A. Dao), bri3tain@skku.edu (Y. Kim), junsin@skku.edu (J. Yi).

https://doi.org/10.1016/j.solmat.2018.12.001
Received 16 July 2018; Received in revised form 27 November 2018; Accepted 1 December 2018
Available online 17 December 2018

collection and anti-reflection is required for the HIT solar cells [6].

Along with the requirements of the opto-electrical properties of TCO films as reported in our previous publication [6], the control of detrimental effects of TCO deposition process on silicon-based underlying layers and hence on surface passivation quality of c-Si also plays a critical role in an achievement of high-efficiency HIT solar cells. Recently, B. Demaurex et al. reported a significant degradation of effective minority carrier lifetime (τ_{eff}) after indium tin oxide (ITO) deposition by direct current (DC) plasma excitation mode at room temperature onto a n-type wafer with 20-nm-thick intrinsic a-Si:H (a-Si:H(*i*)) layers [8]. These authors also presented a small degradation of the τ_{eff} due to luminescence of the sputtering plasma by deposition of ITO films onto the similar cells with a quartz shield [8]. These kinds of degradation were recovered after a few minutes of annealing at 190 °C. Meanwhile, W. Favre et al. reported no degradation of the τ_{eff} at 1-sun illumination of quasi-steady state photoconductance measurement after the ITO deposition at 200 °C [9]. Further, B. M. Meiners et al. presented a different degree of the τ_{eff} degradation between radio frequency (RF) and DC plasma excitation modes after the ITO deposition [10]. No detail explanation, however, was given. A similar phenomenon in the change of the τ_{eff} after the ITO deposition by RF and pulsed DC plasma excitation modes was observed by M. Huang et al. [11]. These authors attributed the different degree of the τ_{eff} degradation between these modes to different energies of the ions towards the sample surface. Meanwhile, A. Illiberi et al. proved that the decrease of surface passivation quality was strongly depended on the ion flux in the argon plasma rather than the ion kinetic energy [12]. All of the above results previously reported by other authors indicated that the ion bombardment, the luminescence of the sputtering plasma, and high-temperature treatment in or after ITO deposition were three factors which mainly affected on the τ_{eff} of the HIT solar cells. These factors have a complicated interaction with each other. It is apparent that various plasma excitation modes have different plasma properties, and hence different ion flux, ion kinetic energies, and luminescence of the sputtering plasma. However, the effects of various plasma excitation modes on the surface passivation quality of the HIT solar cells have not sufficiently reported yet.

In this work, we first investigated the effects of the plasma excitation modes on the surface passivation quality of HIT solar cells through ITO deposition by the RF, RF-superimposed DC, DC, and pulsed DC modes. On the basis of these results, we clarified the origin of the plasma damage to the surface passivation quality under the ITO sputtering. Device simulations also performed to strengthen our argument for the main factor which was dominant in the cell performance under the plasma damage. The changes in the τ_{eff} of the precursor cells using the ITO deposition with various plasma excitation modes at room temperature and 180 °C were compared and discussed to clarify the interaction between the curing step and the plasma damage. The device performance of HIT solar cells was subsequently discussed.

2. Experimental details

ITO films were deposited by various plasma excitation modes such as RF, RF-superimposed DC, DC, and pulsed DC, using the ITO target containing 90 wt% of In_2O_3 and 10 wt% of SnO_2 as a source material. A DC/pulsed-DC power supply and a RF generator simultaneously excited the cathode, which allowed for a continuous control from the DC to the RF mode depending on the power ratio between them. The base pressure of the main chamber and the loading chamber was fixed at 9×10^{-4} Pa and 0.5 Pa, respectively. After reaching the base pressure, a 30-sccm-Ar gas was flowed into the main chamber to maintain the working pressure of 0.2 Pa. The substrate temperature was set at room temperature or 180 °C depending on each investigation. The power density was fixed in four plasma excitation modes. Constant-power mode was used in both DC and pulsed DC cases. The deposition rates of the ITO films deposited by RF, RF-superimposed DC, DC, and pulsed DC are 0.208, 0.220, 0.344, and 0.473 nm/s, respectively. For investigation of opto-electrical properties of the ITO films, the Corning Eagle 2000 glasses were used as substrates.

The resistivity (ρ), carrier concentration (*n*), and Hall mobility (μ) of the ITO films on glass substrates with 20×20 mm^2 in dimension were performed by Hall effect measurement system (Ecopia HMS-3000) using the Van der Pauw geometry at room temperature. The R_{sh} measurements were employed using a four-point probe. The thicknesses of the ITO films were measured by spectroscopic ellipsometry (VASE®, J. A. Woollam). The refractive indices (n_r) and extinction coefficients (k) of the ITO films were also obtained from this measurement. The optical characteristics of the ITO films such as transmittance and reflectance were measured by an integrating sphere of the solar cell spectral response/QE/IPCE measurement system (QEX7). The absorbance of the ITO films was calculated from total transmittance and reflectance spectra.

Commercial n-type Czochralski-grown (Cz) silicon wafers with a crystal orientation of (100), a ρ of 1–10 Ω cm, and a thickness of 200 μm were used as substrates for the fabrication of the HIT solar cells. These wafers were textured and cleaned by a wet-chemical process. To achieve an excellent surface passivation, a-Si:H(*i*) layers were deposited onto both sides of these wafers. A a-Si:H(*n*) layer was deposited onto the front side as a front surface field, whereas a a-Si:H(*p*) layer was deposited onto back side as a rear emitter. More details on the fabricating conditions of these layers can be found elsewhere [13]. To measure the τ_{eff}, precursor cells were fabricated with the a-Si:H(*n*)/a-Si:H(*i*)/c-Si(*n*)/a-Si:H(*i*)/a-Si:H(*p*) structure. Completed cells were employed by the deposition of the ITO films with the foregoing parameters onto the precursor cells through a 10.24-cm^2 metal mask which was directly placed on the a-Si:H(*n*) surface to form active areas. The front and back metal electrodes were prepared by silver paste screen-printing with curing steps at 160 °C in a belt furnace, which corresponded to the 1st and 2nd curing processes in this study, respectively.

The τ_{eff} of the precursor cells and the Suns-V_{oc} of the completed cells were performed by the Quasi-Steady State Photoconductance method (Sinton Consulting, WCT-120). The optical characteristics of the HIT solar cells such as reflectance and external quantum efficiency (EQE) were measured by the solar cell spectral response/QE/IPCE measurement system (QEX7). The device performance was characterized by light current density-voltage under AM 1.5, 100 mWcm^{-2} condition, at 25 °C.

3. Results and discussion

3.1. Analysis of damage to surface passivation quality

As mentioned above, there are three factors which mainly affected on the τ_{eff} of the HIT solar cells: The ion bombardment, luminescence of the sputtering plasma, and process temperature in or after ITO deposition. To eliminate the effect of high temperature on the τ_{eff}, the ITO films were deposited at room temperature. During each ITO deposition, precursor cells with and without the quartz shield were co-deposited to separate the effects of the ion bombardment and the luminescence of the sputtering plasma on the τ_{eff}. Fig. 1(a)–(d) present the τ_{eff} as a function of the excess minority carrier density (Δn) after the ITO deposition at room temperature under various plasma excitation modes and thicknesses. It is apparent that there was a degradation of the τ_{eff} of the precursor cells at both low and high-level injections in all cases after the ITO deposition. This degradation was partly recovered after the 1st and 2nd curing processes. For more details, lifetime ratio defined by a ratio of the τ_{eff} of the precursor cells at 1-sun before and after the ITO deposition was calculated by the following equation and is shown in Fig. 1(e):

$$\tau_{ratio} = 100 \times \frac{\tau_{ITO}}{\tau_{w/o\_ITO}} \quad (1)$$

where τ_{ratio} is the lifetime ratio, τ_{ITO} and τ_{w/o_ITO} are the τ_{eff} of the

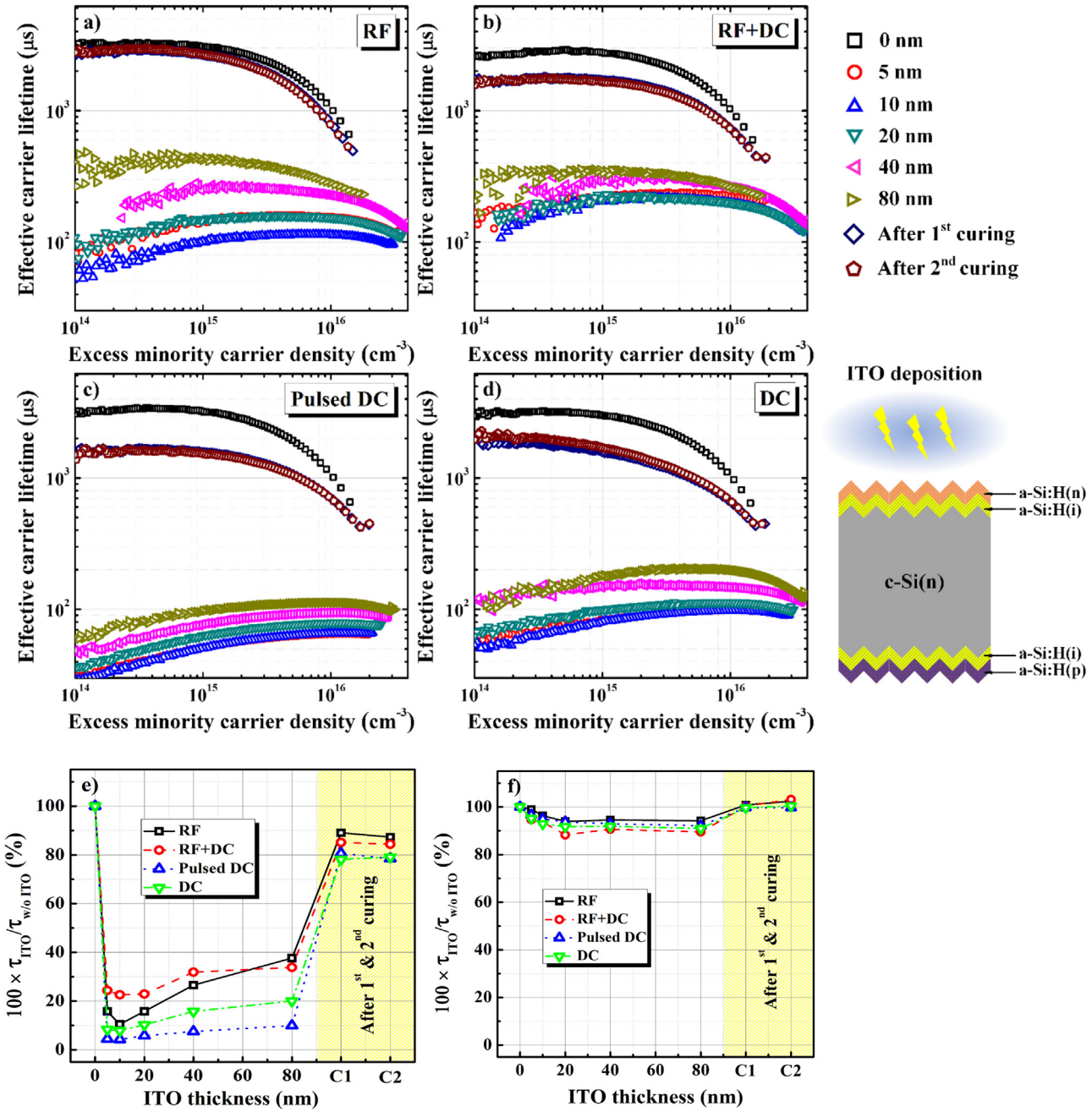

Fig. 1. Effective minority carrier lifetime (τ_{eff}) of the precursor cells after the ITO deposition with various plasma excitation modes as a function of excess minority carrier density: (a) RF, (b) RF-superimposed DC, (c) pulsed DC, and (d) DC. Lifetime ratio of the precursor cells (e) without and (f) with a quartz shield as a function of the ITO film thicknesses with various plasma excitation modes at room temperature. The yellow region presented for the lifetime ratio of precursor cells after the 1st and 2nd curing processes.

precursor cells after and before the ITO deposition, respectively. More than 90% of the τ_{eff} degradation of the precursor cells after the 5-nm-thick ITO films deposited by the pulsed DC and DC plasma excitation modes was observed. Meanwhile, the τ_{eff} of the precursor cells using the ITO films deposited by the RF and RF-superimposed DC plasma excitation modes was less degraded after the ITO deposition with the same thickness. The difference of sputtering damage to surface passivation quality under various plasma excitation modes could correlate with ion flux and ion kinetic energy as well as luminescence of the sputtering plasma. As well known, the energy of incident ions towards the floating sample in the RF plasma excitation mode is much larger than that of incident ions in the DC plasma excitation mode, whereas the ion flux shows an opposite trend with the ion energy [14,15]. The high ion energy in the case of the RF plasma excitation mode is mainly due to the high self-bias voltage between the plasma body and the chamber walls which accelerates the ions approaching the substrate surface [14]. Moreover, A. Illiberi et al. proved that the decrease of surface passivation quality of a-Si/c-Si interface after Ar plasma treatment was strongly depended on the ion flux rather than the ion kinetic energy [12]. Therefore, we attributed the main reason for the degradation of surface passivation contact after the ITO deposition by a sputtering technique to the ion flux in the sputtering plasma rather than the ion kinetic energy.

As also shown in Fig. 1(e), the τ_{eff} was continuously degraded before reaching a minimum value at 20-nm-thick ITO deposition, and slightly improved with a further increase of the ITO thickness. B. Demaurex

et al. also reported a saturated degradation after 20-nm-thick ITO deposition [8]. This was attributed to the protective effect of ITO films against the ion bombardment after reaching a sufficient thickness. The slight improvement of the τ_{eff} could be attributed to the energy transfer of incident ions to the underlying layers that helped to redistribute the hydrogen atoms in the silicon-based layers and near the a-Si/c-Si interface. A significant improvement of the τ_{eff} after 1st and 2nd curing processes was found. This phenomenon was also observed by other reports [8,11,16], and could be expected as the recovery of surface passivation by post-annealing treatment after light-soaking of a-Si/c-Si passivation structure. This curing step, however, could not fully recover the τ_{eff} of precursor cells after ITO deposition at room temperature.

The precursor cells with the quartz shields were co-deposited, and the lifetime ratios of these precursor cells before and after the ITO deposition at room temperature with various plasma excitation modes and thicknesses are shown in Fig. 1(f). The τ_{eff} was slightly degraded before reaching a minimum value at 20-nm-thick ITO deposition and saturated with a further increase of the ITO thickness. The degradation of surface passivation quality in this case was also observed by other reports [8,17]. F. Lebreton et al. also presented a slight degradation of surface passivation quality after Ar plasma treatment [18]. The main reason for such degradation was attributed to the luminescence of the sputtering plasma, i.e. high energy photons in the deep UV range. Interestingly, the τ_{eff} degradation of precursor cells in this case was also stopped at 20-nm-thick ITO deposition. This thickness was exactly equal to the thickness value that was presumed to be sufficient to protect the passivation contact against the ion bombardment. Transmittance spectra of various ITO film thicknesses on quartz were performed to clarify this phenomenon. As shown in Fig. 2, a red-shift of the absorption edges of the ITO films became evident with the increase of the ITO thickness. Such red-shift of the absorption edges eliminated the high energy photons in the deep UV range reaching the precursor cells. A full recovery of the τ_{eff} after 1st and 2nd curing processes was found. The similar explanation for this phenomenon was given above.

As well known, the degradation of surface passivation quality was attributed to the density of interfacial defects (D_{it}) at the a-Si/c-Si interfaces and the defect density of i-layer bulk ($D_{i\text{-}bulk}$). In practice, the ITO films were deposited onto the *p/i* or *n/i* layers. Therefore, the damage of these interfaces and the a-Si:H(*i*) layers by the ITO sputtering was inevitable questioned about the possibility because these interfaces were covered by the *p/i* or *n/i* layers with the total thickness around 12–20 nm. A reduction in the degradation of the τ_{eff} after ITO deposition as the thickness of the a-Si:H layers was increased was observed by B. M. Meiners et al. and A. Tomasi et al. [10,19]. Further, a structural change at the a-Si/c-Si interface after depositing ITO films onto 24-nm-i/c-Si structure observed by the transmission electron microscopy (TEM) was reported by M. Huang et al. [11]. This indicated that the ITO sputtering could damage the a-Si/c-Si interface through a thin enough a-Si:H(*i*) layer, and this layer was also obviously damaged. In general, the thicknesses of the a-Si:H(*i*) layers and the window layers (a-Si:H(*n*) or a-Si:H(*p*)) are kept lower than 10 nm for each layer due to high parasitic absorption of such layers at short-wavelength region, which means that the total thickness of the *p/i* or *n/i* layers is normally lower than 20 nm. In this study, the thicknesses of the a-Si:H(*i*) and window layers (a-Si:H(*n*) or a-Si:H(*p*)) are 5 nm and 10 nm, respectively. Therefore, we strongly believed that with such thin *n/i* layers the ITO sputtering could damage the a-Si/c-Si interfaces and the a-Si:H(*i*) layers. Moreover, we attributed the degradation of surface passivation quality mainly to the damage of the a-Si/c-Si interfaces rather than that of the a-Si:H(*i*) layers.

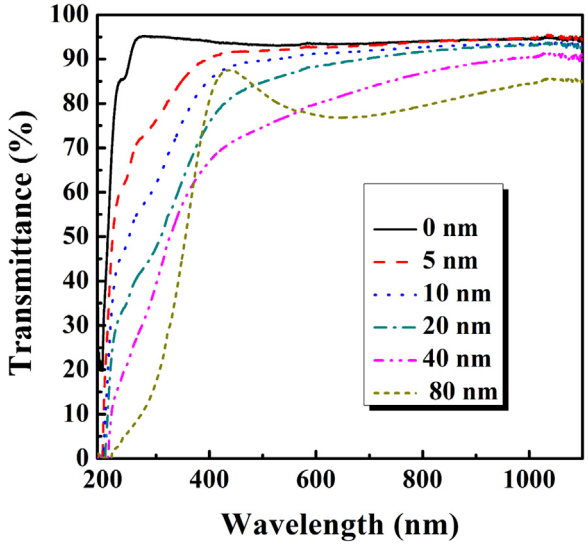

Fig. 2. Total transmittance of the ITO films on the quartz substrate at various thicknesses as a function of the optical wavelength.

To strengthen the above argument, the open-circuit voltage (V_{oc}) of the HIT solar cells as a function of the $D_{i\text{-}bulk}$ and the D_{it} at the a-Si/c-Si interface was investigated by AFORS-HET device simulations and is presented in Fig. 3(a)-(b) [20]. For a comparison, the implied-V_{oc} (iV_{oc}) of the precursor cells obtained from carrier lifetime measurement is also shown in Fig. 3(c). Due to the strong impacts of given ranges of the $D_{i\text{-}bulk}$ and the D_{it} on device performance, these ranges were chosen on the basis of the previous results from the literature [21–23]. Input parameters adopted for HIT solar cells with rear-emitter configuration are shown in Table 1. As shown in Fig. 3(a)-(b), the D_{it} has a dominant impact on the V_{oc} of the HIT solar cells. The V_{oc} was significantly reduced to lower than 620 mV at the D_{it} of 1.5×10^{12} cm^{-2}. Meanwhile, only 35 mV of the V_{oc} was decreased with a remarkable increase of the $D_{i\text{-}bulk}$. It is noteworthy that the iV_{oc} of the precursor cells after 5 nm ITO deposition in the worst case (using the DC mode) was almost similar to the V_{oc} of the HIT solar cells at the highest D_{it} of 1.5×10^{12} cm^{-2}. This indicated that the reduction of the V_{oc} after the ITO sputtering was mainly due to the increase of the D_{it} rather than the degradation of the quality of the a-Si:H(*i*) layers.

Lifetime ratios of the precursor cells after 80-nm-thick ITO films under various plasma excitation modes at room temperature and 180 °C without the quartz shields are shown in Fig. 4. The lifetime ratios of the precursor cells were significantly decreased after the ITO deposition at room temperature, which indicated a remarkable degradation in surface passivation quality. This degradation could only be partially recovered by the 1st and 2nd curing processes. Meanwhile, the lifetime ratios of the precursor cells using the ITO films deposited at 180 °C showed a small degradation in the case of using the DC and pulsed DC modes and a negligible reduction in the case of using the RF and RF-superimposed DC modes. However, there was no significant improvement of lifetime ratio after the 1st and 2nd curing processes. This could be attributed to the lower temperature (160 °C) of curing processes in comparison with that of the ITO deposition (180 °C). This low temperature of the curing processes was intentionally chosen for which it is lower than the substrate temperature of ITO deposition. This is necessary to prevent any possible changes of opto-electrical properties of the ITO films after these curing processes that could impact on cell performance. The small degradation in the case of using the DC and pulsed DC modes and the negligible reduction in the case of using the RF and RF-superimposed DC modes after the ITO deposition at 180 °C could be attributed to a trade-off between degradation and curing step that occurred in the ITO deposition at high temperature. B. Demaurex et al. reported that the degradation of the τ_{eff} of the precursor cells after the ITO deposition at room temperature could be recovered after a few minutes of annealing at 190 °C. Therefore, we strongly believed that the time of the ITO deposition and sequent unloading processes was enough for a curing step.

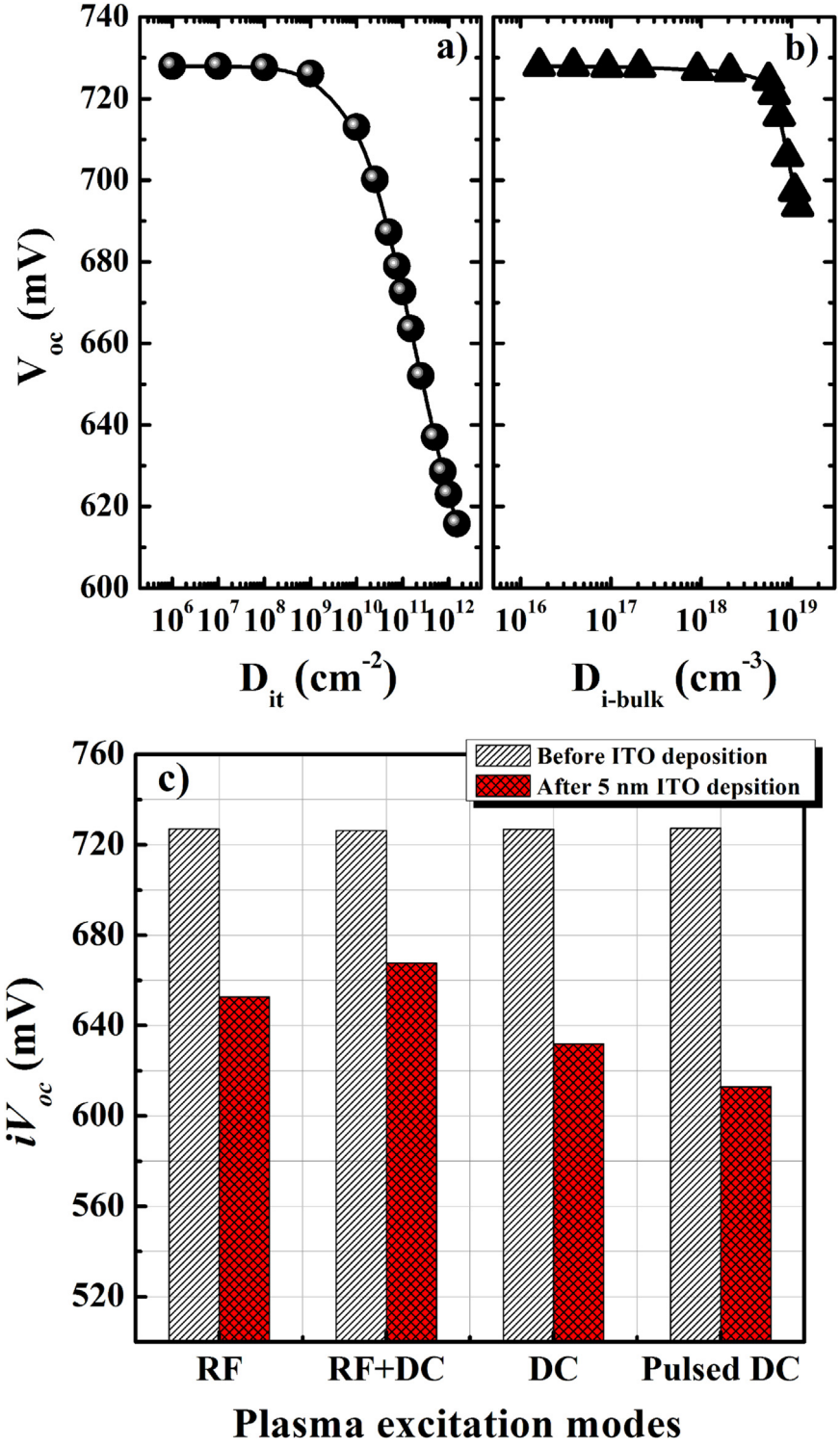

Fig. 3. (a), (b) The open-circuit voltage (V_{oc}) of the HIT solar cells as a function of the D_{it} and the $D_{i\text{-}bulk}$ at the a-Si/c-Si interface performed by AFORS-HET device simulations, respectively; (c) the implied open-circuit voltage (iV_{oc}) of the precursor cells obtained from carrier lifetime measurement.

3.2. Cell performance

The device performance of the HIT solar cells using the ITO films deposited by various plasma excitation modes was obtained by the voltage-current measurement under illumination and is shown in Fig. 5. The highest V_{oc} was obtained from the cells using ITO deposition under RF and RF-superimposed DC, and further decrease with the DC and pulsed DC modes, respectively. This trend was entirely consistent with the trend of the lifetime ratios in Fig. 4(b). The *FF* of the cells showed a different trend. The implied *FF* (*iFF*) of the cells, also known as the pseudo-*FF*, was obtained from the Suns-V_{oc} measurement and is also shown in this figure. The determination of the *iFF* is derived from the τ_{eff} data, and the effects of series resistance are eliminated from it. As shown in Fig. 5, there was a negligible change in the *iFF* of the cells using the ITO deposited by various plasma excitation modes. Meanwhile, the *FF* was increased from the RF mode to RF-superimposed DC

Table 1
Input parameters of AFORS-HET device simulations adopted for HIT solar cells with rear-emitter configuration.

Parameters	a-Si:H(*n*)	a-Si:H(*i*)	a-Si:H(*p*)	c-Si(*n*)
Dielectric constant	11.9	11.9	11.9	11.9
Electron affinity (eV)	3.9	3.9	3.9	4.05
Band gap (eV)	1.71	1.61	1.71	1.124
Optical gap (eV)	1.71	1.61	1.71	1.124
Effective DOS in CB (VB) (cm^{-3})	1×10^{21} (1×10^{21})	1×10^{20} (1×10^{20})	1×10^{20} (1×10^{20})	2.843×10^{19} (2.682×10^{19})
Electron (hole) mobility (cm^2. $V^{-1}.s^{-1}$)	5 (1)	5 (1)	5 (1)	858 (355)
Acceptor doping (cm^{-3})	0	0	3.78×10^{18}	0
Donor doping (cm^{-3})	3.78×10^{18}	0	0	5.63×10^{16}
Thermal velocity of electron (hole) ($cm.s^{-1}$)	1×10^{7} (1×10^{7})	(1×10^{7}) 1×10^{7}	(1×10^{7}) 1×10^{7}	(1×10^{7}) 1×10^{7}
CB (VB) tail Urbach energy (eV)	0.025 (0.03)	0.025 (0.025)	0.035 (0.03)	–
σ_e (σ_h) for CB tail (cm^2)	7×10^{-16} (7×10^{-16})	7×10^{-16} (7×10^{-16})	7×10^{-16} (7×10^{-16})	–
σ_e (σ_h) for VB tail (cm^2)	7×10^{-16} (7×10^{-16})	7×10^{-16} (7×10^{-16})	7×10^{-16} (7×10^{-16})	–
Maximum A-like Gaussian state density (cm^{-3}/eV)	2.51×10^{17}	variation	1.13×10^{17}	–
Maximum D-like Gaussian state density (cm^{-3}/eV)	2.51×10^{17}	variation	1.13×10^{17}	–
Specific energy of Gaussian peak for donor (eV)	0.45	0.7	1.02	–
Specific energy of Gaussian peak for acceptor (eV)	0.65	1	1.2	–
σ_e (σ_h) for A-like Gaussian state (cm^2)	3×10^{-15} (3×10^{-14})	3×10^{-15} (3×10^{-14})	3×10^{-15} (3×10^{-14})	–
σ_e (σ_h) for D-like Gaussian state (cm^2)	3×10^{-14} (3×10^{-15})	3×10^{-14} (3×10^{-15})	3×10^{-14} (3×10^{-15})	–

mode before reaching maximum value with the DC mode and decreased with pulsed DC mode. A different of the trend of the *iFF* and *FF* indicated that the series resistance was dominant in these cells under various plasma excitation modes of the ITO deposition.

To clarify the trend of the *FF*, the electrical properties of the ITO films deposited by various plasma excitation modes were obtained from the Hall effect measurement and the four-point probe. As shown in Fig. 6, the n was increased from the RF mode to the RF-superimposed DC mode before reaching maximum value with the DC mode and decreased with the pulsed DC mode. Meanwhile, the μ showed an opposite trend. The highest μ of 55.26 cm^2 $V^{-1}.s^{-1}$ was obtained from the pulsed DC mode. The trend of the ρ and the R_{sh} of ITO films was a result of the trade-off between the n and μ via the following equations:

$$\rho = \frac{1}{en\mu} \tag{2}$$

$$R_{sh} = \frac{\rho}{t} \tag{3}$$

where t is the thickness of the ITO films. As mentioned above, due to the low conductivity of doped a-Si layers, the lateral conductivity of the ITO films plays a critical role in carrier collection. In a screen-printed HIT solar cell, the charge carriers were passed through the ITO films before being collected by metallic fingers with millimeter-spacing.

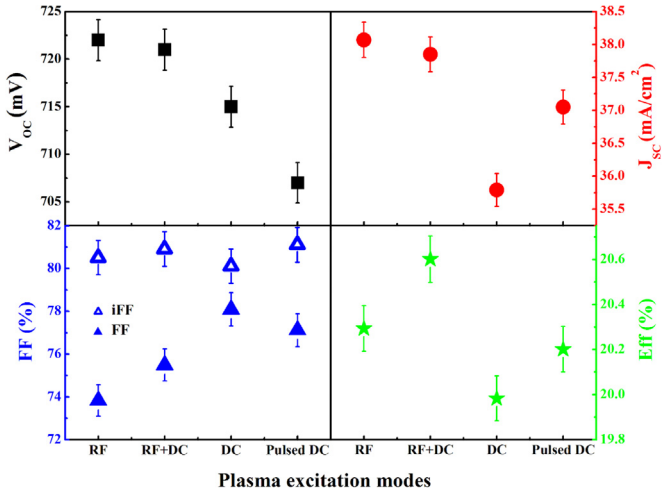

Fig. 5. J-V characteristics under illumination of the HIT solar cells using the ITO films deposited under various plasma excitation modes.

Therefore, the power loss due to Joule heating during this collection process is proportional to the R_{sh} of ITO films. The R_{sh} was decreased from the RF mode to the RF-superimposed DC mode before reaching

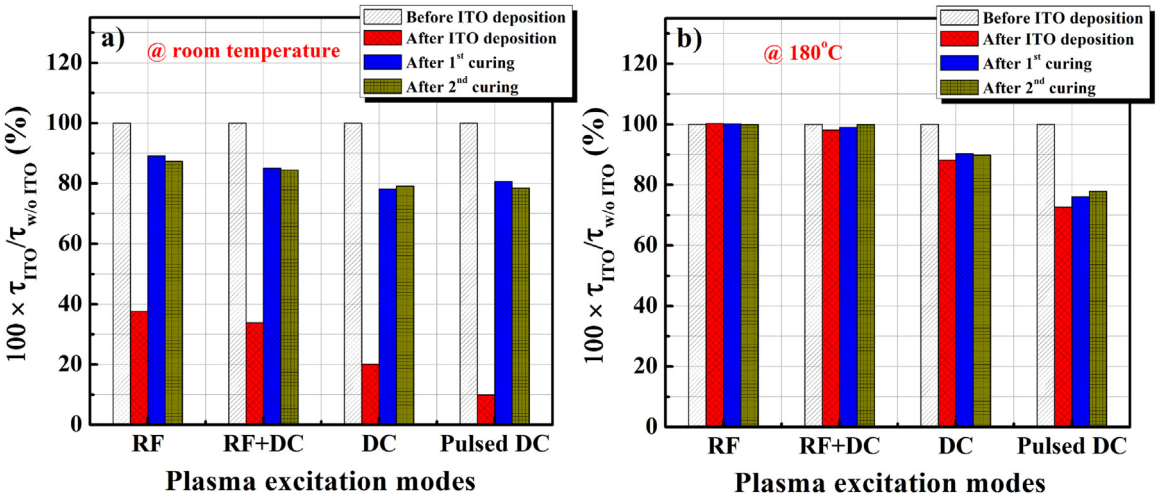

Fig. 4. Lifetime ratios of precursor cells using the ITO films under various plasma excitation modes at (a) room temperature, and (b) 180 °C without the quartz shields.

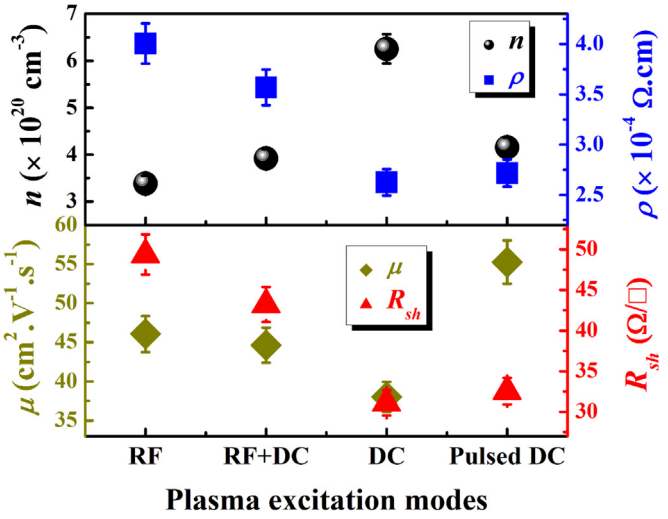

Fig. 6. The carrier concentration (n), Hall mobility (μ), resistivity (ρ), and sheet resistance (R_{sh}) of the ITO films deposited by various plasma excitation modes.

minimum value with the DC mode and slightly increased with the pulsed DC mode. This trend was entirely consistent with the trend of the *FF* of the cells.

Fig. 5 also depicts the optical parameter of the cells, J_{sc}. The J_{sc} was slightly decreased from the RF mode to the RF-superimposed DC mode before significantly reducing with the DC mode, and increased with the pulsed DC mode. To clarify the trend of the J_{sc}, the optical properties of the cells and the ITO films deposited by various plasma excitation modes, were measured by the solar cell spectral response/QE/IPCE system. As shown in Fig. 7(a), the EQE spectra of the cells using the ITO films deposited by the RF and RF-superimposed DC modes showed a negligible difference. Meanwhile, the EQE spectra of the cells using the ITO films deposited by the DC and pulsed DC modes exhibited a significant reduction in the visible and near-infrared (NIR) region. In the short wavelength region, there was a negligible change in the EQE spectra. This phenomenon could be interpreted after analyzing the cell reflectance and the optical properties of the ITO films. As shown in Fig. 7(b), the order of the cell reflectance was $R_{RF} < R_{RF+DC} < R_{Pulsed\ DC} < R_{DC}$ and the cell reflectance was decreased in the whole wavelength range. This was mainly due to a similar reduction of the n_r of the ITO films, as shown in Fig. 7(c). In particular, a significant reduction of the n_r of the ITO films deposited by the DC mode at the NIR region was observed. This was mainly due to a high n of these ITO films, as shown in Fig. 6. Fig. 7(d) shows the absorbance of the ITO films deposited by various plasma excitation modes. Interestingly, the absorbance of these ITO films in the short wavelength region showed an opposite trend with the cell reflectance: $A_{RF} > A_{RF+DC} > A_{Pulsed\ DC} > A_{DC}$. This was mainly due to the trend of the n of the ITO films that impacted on the shift of

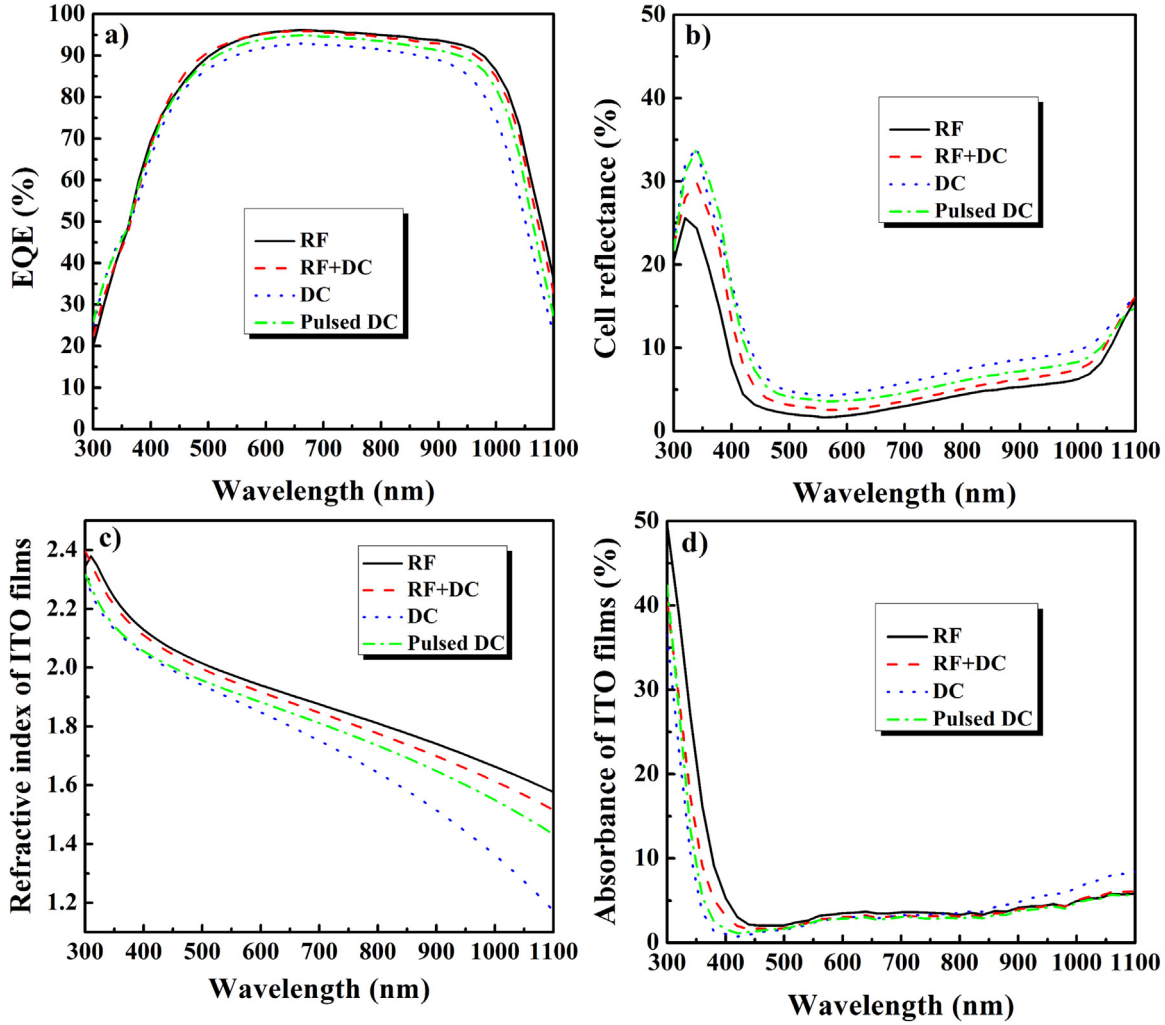

Fig. 7. (a) EQE spectra, and (b) reflectance of the HIT solar cells; (c) refractive index, and (d) absorbance of the ITO films deposited by various plasma excitation modes.

the absorption edge, known as the Burstein-Moss effect [24]. Therefore, the negligible change in the EQE spectra at the short wavelength region was due to the trade-off between the cell reflectance and the parasitic absorption of the ITO films. The trend of the EQE spectra in the visible and NIR region followed that of the cell reflectance.

Finally, the η of cells is also presented in Fig. 5. Due to the trade-off between the V_{oc}, J_{sc}, and *FF*, the highest η of 20.6% was obtained from the RF-superimpose DC modes, whereas the cells using the ITO films deposited by DC mode showed the lowest η. To our best knowledge, this is the first time that the ITO films deposited by the RF-superimpose DC mode are used as electrodes in the HIT solar cells. Our results showed that the ITO films deposited by RF-superimposed DC exhibited a high potential as excellent opto-electrical properties and free sputter-induced damage electrodes for HIT solar cell applications.

4. Conclusion

The damage to passivation contact by ITO sputtering under various plasma excitation modes such as RF, RF-superimposed DC, DC, pulsed DC, and its impacts on cell performance are presented. Regardless of plasma excitation modes, a remarkable degradation of the τ_{eff} of the precursor cells after the ITO deposition at room temperature was observed. We attributed the main reason for this degradation after the ITO deposition by a sputtering technique to the ion flux in the sputtering plasma rather than the ion kinetic energy. We also found that the degradation of surface passivation quality was mainly due to the damage of the a-Si/c-Si interfaces rather than that of the a-Si:H(*i*) layers. For the ITO deposition at 180 °C, no degradation of the τ_{eff} in the case of using the RF and RF-superimposed DC and small degradation of the τ_{eff} in the case of using the DC and pulsed DC were found. These were attributed to the trade-off between degradation and curing step that occurred in ITO deposition at a high temperature. The cell performance of the HIT solar cells using the ITO films deposited by various plasma excitation modes at 180 °C was performed. The trend of the V_{oc} of the cells was entirely consistent with that of the lifetime ratios of the precursor cells. On the basis of the cell performance, the ITO films deposited by the RF-superimposed DC exhibited a high potential as excellent opto-electrical properties and free sputter-induced damage electrodes for HIT solar cell applications.

Acknowledgments

This research is funded by Vietnam National Foundation for Science and Technology Development (NAFOSTED) under grant number 103.02-2017.43. This work was also supported by the New & Renewable Energy Core Technology Program of the Korea Institute of Energy Technology Evaluation and Planning (KETEP), granted financial resource from the Ministry of Trade, Industry & Energy, Republic of Korea (No. 20163010012230).

References

[1] S. Almosni, A. Delamarre, Z. Jehl, D. Suchet, L. Cojocaru, M. Giteau, B. Behaghel, A. Julian, C. Ibrahim, L. Tatry, Material challenges for solar cells in the twenty-first century: directions in emerging technologies, Sci. Technol. Adv. Mater. 19 (2018) 336–369.

[2] A.H.T. Le, S. Ahn, S. Han, J. Kim, S.Q. Hussain, H. Park, C. Park, C.P.T. Nguyen, V.A. Dao, J. Yi, Effective optimization of indium tin oxide films by a statistical approach for shallow emitter based crystalline silicon solar cell applications, Sol. Energy Mater. Sol. Cells 125 (2014) 176–183.

[3] J. Zhao, A. Wang, M.A. Green, 24·5% Efficiency silicon PERT cells on MCZ substrates and 24·7% efficiency PERL cells on FZ substrates, Progress. Photovolt.: Res. Appl. 7 (1999) 471–474.

[4] K. Masuko, M. Shigematsu, T. Hashiguchi, D. Fujishima, M. Kai, N. Yoshimura, T. Yamaguchi, Y. Ichihashi, T. Mishima, N. Matsubara, Achievement of more than 25% conversion efficiency with crystalline silicon heterojunction solar cell, IEEE J. Photovolt. 4 (2014) 1433–1435.

[5] K. Yoshikawa, H. Kawasaki, W. Yoshida, T. Irie, K. Konishi, K. Nakano, T. Uto, D. Adachi, M. Kanematsu, H. Uzu, Silicon heterojunction solar cell with interdigitated back contacts for a photoconversion efficiency over 26%, Nat. Energy 2 (2017) 17032.

[6] A.H.T. Le, S. Ahn, S. Kim, S. Han, S. Kim, H. Park, C.P.T. Nguyen, V.A. Dao, J. Yi, A statistical approach for the optimization of indium tin oxide films used as a front contact in amorphous/crystalline silicon heterojunction solar cells, Energy Convers. Manag. 87 (2014) 191–198.

[7] S. Dhar, S. Mandal, G. Das, S. Mukhopadhyay, P.P. Ray, C. Banerjee, A.K. Barua, Silicon heterojunction solar cells with novel fluorinated n-type nanocrystalline silicon oxide emitters on p-type crystalline silicon, Jpn. J. Appl. Phys. 54 (2015) 08KD03.

[8] B. Demaurex, S. De Wolf, A. Descoeudres, Z. Charles Holman, C. Ballif, Damage at hydrogenated amorphous/crystalline silicon interfaces by indium tin oxide overlayer sputtering, Appl. Phys. Lett. 101 (2012) 171604.

[9] W. Favre, J. Coignus, N. Nguyen, R. Lachaume, R. Cabal, D. Munoz, Influence of the transparent conductive oxide layer deposition step on electrical properties of silicon heterojunction solar cells, Appl. Phys. Lett. 102 (2013) 181118.

[10] B.-.M. Meiners, S. Holinski, P. Schäfer, S. Hohage, D. Borchert, Sputter damage to amorphous silicon layers for heterojunction solar cells, in: Proceedings of the 31st European PV Solar Energy Conference and Exhibition (EU PVSEC. 2015), Hamburg, Germany, 2015.

[11] M. Huang, Z. Hameiri, A.G. Aberle, T. Mueller, Comparative study of amorphous indium tin oxide prepared by pulsed-DC and unbalanced RF magnetron sputtering at low power and low temperature conditions for heterojunction silicon wafer solar cell applications, Vacuum 119 (2015) 68–76.

[12] A. Illiberi, P. Kudlacek, A. Smets, M. Creatore, M. Van De, Sanden, Effect of ion bombardment on the a-Si:H based surface passivation of c-Si surfaces, Appl. Phys. Lett. 98 (2011) 242115.

[13] S. Kim, V.A. Dao, Y. Lee, C. Shin, J. Park, J. Cho, J. Yi, Processed optimization for excellent interface passivation quality of amorphous/crystalline silicon solar cells, Sol. Energy Mater. Sol. Cells 117 (2013) 174–177.

[14] M. Bender, J. Trube, J. Stollenwerk, Characterization of a RF/dc-magnetron discharge for the sputter deposition of transparent and highly conductive ITO films, Appl. Phys. A 69 (1999) 397–401.

[15] R. Cebulla, R. Wendt, K. Ellmer, Al-doped zinc oxide films deposited by simultaneous rf and dc excitation of a magnetron plasma: relationships between plasma parameters and structural and electrical film properties, J. Appl. Phys. 83 (1998) 1087–1095.

[16] A. Morales-Vilches, C. Voz, M. Colina, G. López, I. Martín, P. Ortega, A. Orpella, R. Alcubilla, Recovery of indium-tin-oxide/silicon heterojunction solar cells by thermal annealing, Energy Procedia 44 (2014) 3–9.

[17] D. Skorka, N. Brinkmann, A. Gorgulla, G. Hahn, B. Terheiden, Changes in passivation quality of PECV-deposited hydrogenated amorphous silicon layers used in solar cells due to sputter deposition of TCOs, in: 28th European Photovoltaic Solar Energy Conference and Exhibition, 2013, pp. 1162–1165.

[18] F. Lebreton, S. Abolmasov, F. Silva, P. Roca, i Cabarrocas, In situ photoluminescence study of plasma-induced damage at the a-Si: h/c-si interface, Appl. Phys. Lett. 108 (2016) 051603.

[19] A. Tomasi, F. Sahli, J.P. Seif, L. Fanni, S.M. de Nicolas Agut, J. Geissbühler, B. Paviet-Salomon, S. Nicolay, L. Barraud, B. Niesen, Transparent electrodes in silicon heterojunction solar cells: influence on contact passivation, IEEE J. Photovolt. 6 (2016) 17–27.

[20] R. Varache, C. Leendertz, M. Gueunier-Farret, J. Haschke, D. Muñoz, L. Korte, Investigation of selective junctions using a newly developed tunnel current model for solar cell applications, Sol. Energy Mater. Sol. Cells 141 (2015) 14–23.

[21] M. Stutzmann, The defect density in amorphous silicon, Philos. Mag. B 60 (1989) 531–546.

[22] B. Bahardoust, N. Kherani, S. Costea, D. Yeghikyan, S. Zukotynski, Defect density in doped amorphous layer and interface of silicon heterojunction devices obtained with the constant photocurrent method (in: Photovoltaic Energy Conversion, Conference Record of the 2006 IEEE 4th World Conference on), IEEE, 2006, pp. 1187–1190 (in: Photovoltaic Energy Conversion, Conference Record of the 2006 IEEE 4th World Conference on).

[23] C. Zhong, R. Yao, K. Geng, Characterization of interface states in a-Si: h/c-si heterojunctions by an expression of the theoretical diffusion capacitance, J. Phys. D: Appl. Phys. 43 (2010) 495102.

[24] E. Burstein, Anomalous optical absorption limit in InSb, Phys. Rev. 93 (1954) 632.